Mechanism for island formation during low-temperature growth on (100) surfaces of fcc metals

Marinus Breeman, Georg Rosenfeld, and George Comsa
Institut für Grenzflächenforschung und Vakuumphysik, Forschungszentrum Jülich, D-52425 Jülich, Germany
(Received 23 July 1996)

We propose a mechanism for island formation during growth on (100) surfaces of fcc metals in the absence of both thermal and nonthermal mobility of isolated adatoms: the rearrangement of atoms in islands by local diffusion processes. By means of kinetic Monte Carlo simulations we investigate the influence of these diffusion processes on the growth properties. For all these allowed rearrangement processes one single hopping rate H was chosen. For H smaller than the deposition rate R the influence of the diffusion is negligible, in the sense that the surface morphology is hardly distinguishable from the case $H=0$. For larger values of H/R island formation is observed, with an average island separation of 7–8 interatomic distances, in reasonable agreement with experiments. [S0163-1829(96)08448-2]

In recent years considerable progress in understanding the role of the fundamental processes occurring during the early stages of homoepitaxial growth has been obtained with the help of experimental techniques (high-resolution microscopy and diffraction techniques) and theoretical developments (computer simulations and analytical theory). There remain, however, a number of problems which are not yet fully understood. One of these problems is outlined below. It is well known that during growth at temperatures where thermally activated mobility of isolated adatoms is sufficiently high, islands are formed on the surface.[1] These islands have a characteristic separation, which may be accessed by real-space methods like scanning tunneling microscopy (STM), but also by diffraction methods like low-energy electron diffraction[2,3] (LEED) or thermal-energy atom scattering (TEAS).[4] However, island formation is also observed in cases where thermally activated isolated-adatom diffusion is assumed to be completely suppressed. For example, for Cu/Cu(100) at 120 K Ernst and co-workers concluded from a peak-profile analysis of their TEAS measurements that an interisland spacing of approximately 14 interatomic distances was present on the surface.[4] For the same system at 77 K Nyberg, Kief, and Engelhoff found a value of 10 interatomic distances with LEED.[3] They also found the same value of 10 interatomic distances for Fe/Cu(100) at 77 K.[3] In order to explain island formation in the absence of *thermal* isolated-adatom mobility posibilities for *nonthermal* mobility were considered. Nyberg and co-workers proposed[3] that transient mobility (i.e., the deposited atoms use part of their condensation energy to make a few jumps on the surface[5]) is responsible for the experimentally observed island formation. In this paper we propose an alternative explanation for island formation in the *absence* of both thermal and nonthermal (transient) isolated-adatom mobility: the rearrangement of island atoms by local diffusion processes. We define an isolated adatom as an adatom which has no in-plane neighbors (neither nearest nor next nearest). We use kinetic Monte Carlo simulations to study the island formation process, and to characterize the influence of these diffusion processes on the growth properties.

The basic assumption in our model is that on (100) surfaces of fcc metals local rearrangement of atoms in (small) islands is possible, even at temperatures where isolated adatoms cannot move. As a consequence of this assumption diffusion of atoms along island edges (configuration A in Fig. 1) is possible. The assumption that on (100) surfaces of fcc metals diffusion along close-packed step edges has a lower activation energy than isolated-adatom hopping is supported by atomistic calculations for various systems.[6,7] We expect this assumption to be valid for systems for which atomic hopping is the relevant isolated-adatom diffusion mechanism, rather than an exchange process. Hopping is certainly not favored on all (100) surfaces. Indeed, from calculations[8] and experiments[9] it is known that on the (100) planes of Al, Ir, and Pt exchange diffusion is favored over atomic hopping. However, at least for Ag on Ag(100) it is known that atomic hopping is the most favorable diffusion mechanism.[7] The assumption that for fcc metals, for which adatom diffusion on terraces occurs by atomic hopping, edge diffusion along close-packed steps has a lower activation energy than isolated-adatom diffusion on terraces is supported by a simple argument involving the coordination number of a diffusing atom. As shown in Fig. 2(a), in its initial state an isolated adatom on the terrace has four nearest neighbors (NN's). In the transition state of an atomic hop over a bridge site it has only two NN's [Fig. 2(b)], resulting in a coordination loss of two NN's. An adatom attached to a close-packed step edge has five NN's in its initial state [Fig. 2(c)]. In the transition state of an atomic jump along the step it still has four NN's left [Fig. 2(d)], resulting in a coordination loss of only one NN. Therefore, it is likely that the activation energy for step-edge diffusion is lower than the energy barrier for isolated-adatom diffusion by hopping. Following this line of reasoning, we also allow the diffusion processes B to F in Fig. 1 in our simulations. All other diffusion processes, including isolated-adatom diffusion, were forbidden. For simplicity, we have chosen a unique hopping rate H for all allowed diffusion processes.

In our kinetic Monte Carlo simulations we used a 100×100 square lattice, with periodic boundary conditions parallel to the surface plane. A simulation consists of a sequence of moves from one configuration to another. A move is either the deposition of an atom, or the jump of an atom to a vacant nearest-neighbor site. For each configuration a list

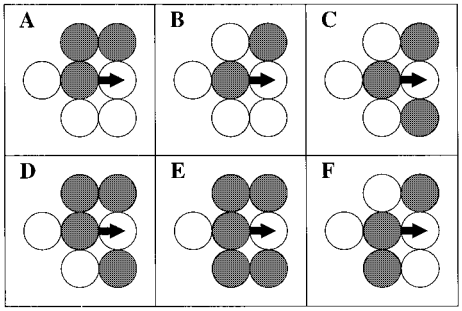

FIG. 1. Sketch of the allowed diffusion processes. The black atom makes a jump to the right (indicated by the arrow). White circles are empty sites, and gray circles are occupied sites. The occupancy of the atomic sites which are not drawn is not important.

of all possible moves is made. One of these moves is selected and executed. The probability for a move to be selected is proportional to the rate of that specific move. After execution of the selected move the simulation time is incremented by the inverse of the sum of all rates of all possible moves for the given configuration. In the simulations presented in this paper we deposited the equivalent of 5 ML. Atoms were deposited at random with a deposition rate R ML/s. A fourfold hollow site with all four atomic sites below occupied is considered a stable adsorption site. Deposition at sites where at least one of the four atoms below is missing leads to ''downward funneling:''[10] the deposited atom falls into a vacancy below until it reaches a stable adsorption site. Thermally activated interlayer diffusion was not allowed. We studied the influence of the allowed diffusion processes on the growth properties and surface morphology by variation of the ratio H/R between 0 and 10^5. For each value of H/R we performed 50 simulations, in order to reduce statistical errors.

Figure 3 shows snapshots of the simulations for four different H/R values after deposition of 0.5 ML. As can be seen in this figure, the surface morphology for $H/R=1$ is hardly different from the case $H/R=0$ (no diffusion). For higher values of H/R, however, substantial changes in the surface morphology are observed: more or less compact structures (islands) are formed, even though—remember—isolated-adatom diffusion on terraces is absent. In Fig. 4 we show an example of how the diffusion processes which are allowed in our simulations can lead to the formation of compact islands.

In order to compare our simulation results with experiments we calculated for the various simulated H/R values the peak profiles of the specular peak by taking the Fourier

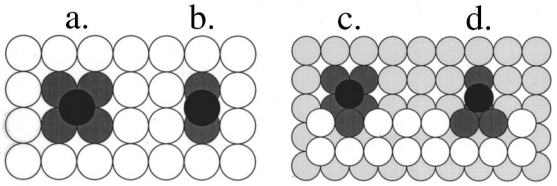

FIG. 2. Sketch of the coordination before and during an atomic jump. (a) Initial state and (b) transition state of an isolated adatom, (c) initial state and (d) transition state of an adatom attached to a close-packed step. The black atom is the diffusing adatom, and its nearest neighbors are drawn in gray.

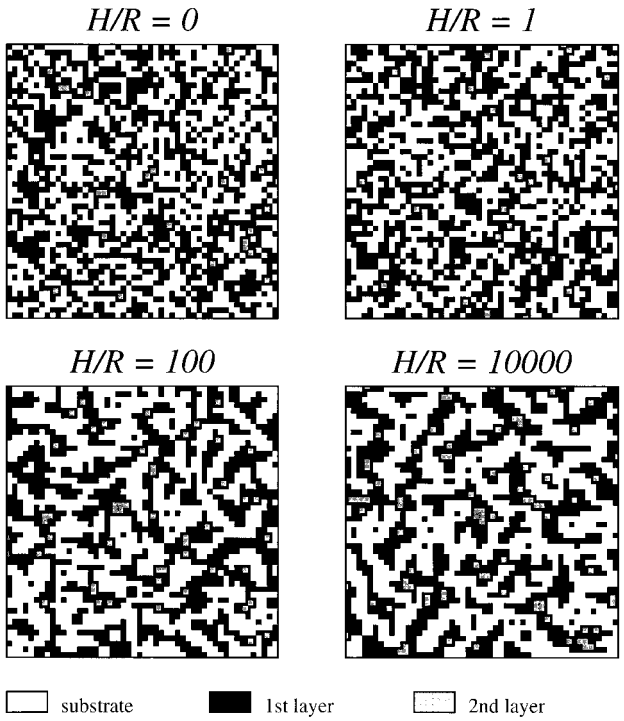

FIG. 3. Snapshots of the simulations after deposition of 0.5 ML for H/R equal to (a) 0, (b) 1, (c) 100, and (d) 10 000.

transform of the pair-pair correlation function. The peak profiles were calculated for a coverage of 0.5 ML. The circularly averaged profiles are shown in Fig. 5. In case a characteristic island separation is present on the surface, satellite peaks to the main diffraction peak should be visible. From the distance between the satellite peak and the main peak the average island separation can be determined. As can be seen in Fig. 5, for low values of H/R no satellite peaks are present. However, for higher values ($H/R>100$), which correspond[11] to the experimental situation in Refs. 4 and 3, clear satellite peaks are visible. The position of these satellite peaks in reciprocal space corresponds to a real-space interisland separation of seven to eight interatomic distances, almost independent of H/R. In view of the simplicity of the simulation model used here, this value is in reasonable

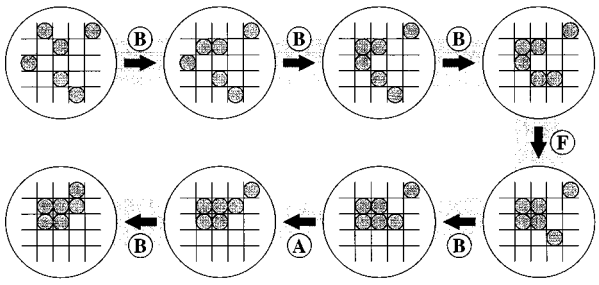

FIG. 4. Example of how the allowed diffusion processes can lead to the formation of compact structures. It takes seven steps to go from the configuration shown in the upper left corner, where no atom has a nearest neighbor, to the configuration shown in the lower left corner. The labels of the arrows connecting successive configurations describe the type of diffusion process according to Fig. 1.

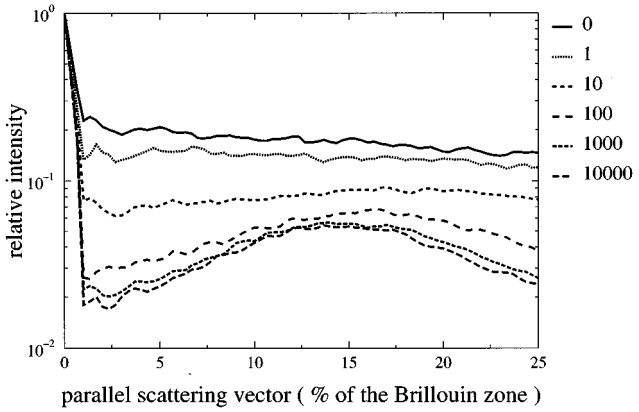

FIG. 5. Diffraction-peak profiles after deposition of 0.5 ML for various values of H/R.

agreement with the values observed in LEED (Ref. 3) and TEAS (Ref. 4) experiments. This shows that islands with the experimentally observed separation are, indeed, created in the absence of thermal and nonthermal mobility of isolated adatoms, if only rearrangements are allowed.

The presence of compact structures in a layer leads to an increase in the number of stable adsorption sites in the next-higher layer. Consequently, the partial coverage of this higher layer will be larger than for cases where no or less compact structures are present. This can be clearly seen from a comparison of the second-layer coverages for the cases $H=0$ and $H=10\,000$ in Fig. 3. Since the tendency to form compact structures is not limited to the first layer, it is to be expected that large values of H/R will result in the growth of rougher layers.

We can quantify the film roughness by calculating the interface width W.[12] This quantity is defined by $W^2=\Sigma(i-\theta)^2N(i)$, where θ is the total coverage, and $N(i)$ is the exposed coverage of layer i: $N(i)=C(i)-C(i+1)$, where $C(i)$ is the coverage in layer i. The summation extends over all layers. In Fig. 6 we plotted the interface width during deposition of the first five ML's for various values of H/R. It is clear from this graph that the surface roughness increases monotonically with increasing H/R. The derivative of the surface roughness with respect to H/R is small for $H/R<1$ and for $H/R>1000$, and shows a maximum for H/R in the range 10–100.

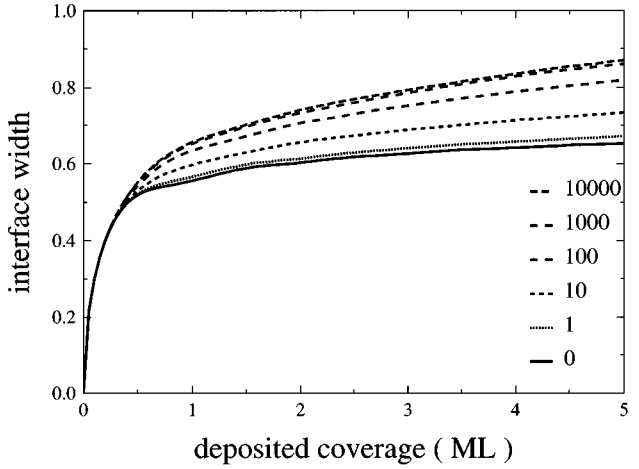

FIG. 6. Interface width (see text) during deposition of 5 ML for various values of H/R, as indicated.

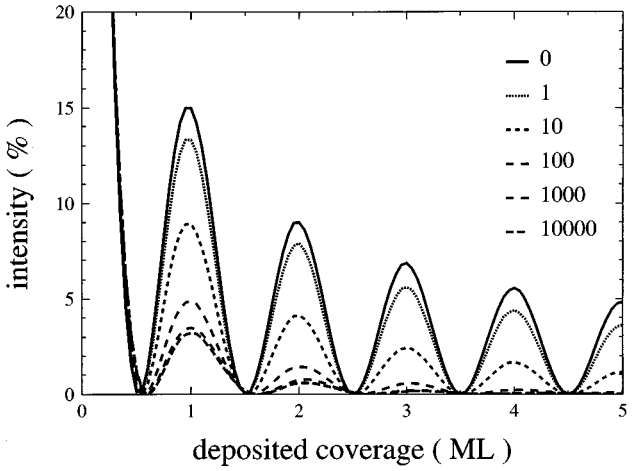

FIG. 7. Anti-Bragg intensity during deposition of 5 ML for various values of H/R, as indicated.

One way to obtain information about the growth mode and surface roughness during growth is to measure the specularly reflected intensity in antiphase scattering conditions by means of a diffraction method. In Fig. 7 we plotted the antiphase intensity during deposition of the first five ML's for various values of H/R. The intensities are calculated in the kinematic approximation, and assuming an ideal instrument. These results should be interpreted as follows. In case the growth mode is close to layer-by-layer growth, oscillations with a period of one ML are observed in the specular intensity. In the case of ideal layer-by-layer growth the intensity in the maxima of the oscillations is equal to the initial intensity. A deviation from ideal layer-by-layer growth results in a damping of the amplitude of the oscillations. The larger the deviation from layer-by-layer growth (i.e., the rougher the growth) the lower the maxima and the larger the damping. When the growth mode is nearly perfectly three-dimensional (Poisson growth) no oscillations are visible, and the specularly reflected intensity decreases monotonically during deposition. As can be seen in Fig. 7, oscillations (indicating quasi-layer-by-layer growth) are present for all values of H/R. The quality of the oscillations changes as a function of H/R: the amplitude of the oscillations decreases, and the damping of the oscillations increases with increasing H/R. These results confirm the statement that more compact structures (higher H/R values) result in rougher films. The fact that we observe growth oscillations is a direct consequence of the implementation of the ''downward funneling'' effect in our simulations. Evans *et al.* showed that in case this mechanism is operative, growth oscillations are visible during low-temperature growth.[10] They attributed the experimental observation of low-temperature growth oscillations[5] to this effect.

In conclusion, we have shown that local diffusion processes lead to island formation during growth on (100) surfaces of fcc metals, even when both thermal and nonthermal isolated-adatom mobility are absent. The influence of these local diffusion processes on the growth properties was studied by means of kinetic Monte Carlo simulations. In our

simulations, we assumed all allowed diffusion processes to have the same hopping rate H. For $H/R>10$ we observed the formation of compact structures (islands) on the surface. Calculated peak profiles of the specular peak revealed satellite peaks for $H/R>100$. From the position of these satellite peaks a characteristic island separation of seven to eight interatomic distances was found, in reasonable agreement with experimental data obtained for metal-on-metal systems at low temperatures. The average island separation was found to be almost independent of H/R. The presence of compact structures on the surface leads to larger partial coverages in higher layers, resulting in the growth of rougher films. This was demonstrated by the monotonic increase with H/R of the interface width. We also calculated the antiphase intensity during deposition of the first five ML's. For increasing values of H/R this quantity showed lower maxima and stronger damping, indicating rougher growth. Our simulation study provides a simple model, including ''downward funneling'' and local diffusion processes, which qualitatively explains experimental observations for low-temperature growth on the (100) surfaces of fcc metals. On (111) surfaces of fcc metals this mechanism for island formation during growth at low temperatures is presumably not operative. The presence of dendritic islands in low-temperature growth experiments on these surfaces[13–15] indicates that on (111) surfaces the formation of compact structures by local rearrangement of atoms in islands is inhibited at low temperatures.

M.B. thanks the Alexander von Humboldt Foundation for support.

[1] J.A. Venables, Philos. Mag. **27**, 697 (1973); J.A. Venables, G.D.T. Spiller, and M. Hanbrücken, Rep. Prog. Phys. **16**, 399 (1984).
[2] J.-K. Zuo *et al.*, Phys. Rev. Lett. **72**, 3064 (1994).
[3] G.L. Nyberg, M.T. Kief, and W.F. Egelhoff, Jr., Phys. Rev. B **48**, 14 509 (1993).
[4] H.J. Ernst, F. Fabre, and J. Lapujoulade, Phys. Rev. B **46**, 1929 (1992).
[5] W.F. Egelhoff, Jr. and I. Jacob, Phys. Rev. Lett. **62**, 921 (1989).
[6] See, e.g., A.F. Voter, Phys. Rev. B **34**, 6819 (1986); M. Breeman, G.T. Barkema, and D.O. Boerma, Surf. Sci. **303**, 25 (1994); J. Merikosi and T. Ala-Nissila, Phys. Rev. B **52**, R8715 (1995).
[7] B.D. Yu and M. Scheffler, Phys. Rev. Lett. **77**, 1095 (1996).
[8] P.J. Feibelman, Phys. Rev. Lett. **65**, 729 (1990).
[9] G. Kellogg and P.J. Feibelman, Phys. Rev. Lett. **64**, 3143 (1990); C. Chen and T.T. Tsong, *ibid.* **64**, 3147 (1990).
[10] J.W. Evans *et al.*, Phys. Rev. B **41**, 5410 (1990).
[11] With typical values for activation energy (0.25 eV), attempt frequency (10^{13} Hz), temperature (100 K), and deposition rate (10^{-2} ML/s), $H/R\sim 260$.
[12] M. Thomsen and A. Madhukar, J. Cryst. Growth **80**, 275 (1987).
[13] M. Bott, Th. Michely, and G. Comsa, Surf. Sci. **272**, 161 (1992).
[14] G. Rosenfeld *et al.*, Phys. Rev. Lett. **71**, 895 (1993).
[15] W. Wulfhekel *et al.*, Surf. Sci. **348**, 227 (1996).